Desalination and Water Treatment
www.deswater.com

doi: 10.5004/dwt.2017.20872

96 (2017) 153–160
November

Enhanced photocatalytic mechanism of hydroxyl radical formation in the composite reaction of TiO_2/oxidant for azo dye degradation

Jyun-Hong Shen[a,*], Hung-Yi Chuang[b], Jao-Jia Horng[b]

[a]*Graduate School of Engineering Science and Technology, National Yunlin University of Science and Technology (YunTech), Yunlin 64002, Taiwan, Tel. +886 5 534 2601; email: cgh1210@gmail.com*
[b]*Department of Safety, Health and Environmental Engineering, Yunlin 64002, Taiwan, emails: james710404@gmail.com (H.-Y. Chuang), horngjj@gmail.com (J.-J. Horng)*

Received 23 December 2016; Accepted 25 April 2017

ABSTRACT

In order to improve visible light-driven photocatalytic activity, two oxidants, potassium dichromate (Cr(VI)) and potassium permanganate (Mn(VII)) were combined with TiO_2 photocatalysis for the degradation of dye acid orange 7 (AO7). The assessments of photocatalytic activity including AO7 mineralization and hydroxyl radical (•OH) formation were measured by total organic carbon and coumarin probing with fluorescence, respectively. Based on the assessed results varied with different irradiation wavelengths and dissolved oxygen levels, the parametric effects and •OH formation trends were estimated to further propose the possible mechanisms. A highly positive correlation (r = 0.82) between AO7 mineralizations and •OH formations was observed. The •OH formation trends from valence band (VB) and conduction band (CB) sites on TiO_2 were nearly similar under ultraviolet irradiation, while those under visible irradiation were uneven (34% and 66% for VB and CB sites, respectively). Owing to the fact that Cr(VI) and Mn(VII) are electron acceptors, the total •OH formations were enhanced to 126% and 144% by increasing the utilization of original photogenerated electrons with their redox reactions. In the meantime, the hole–electron recombination could also be inhibited to benefit the photodegradation of AO7. This mechanism was slightly different from the general strategies for improvement of photocatalytic activity.

Keywords: Visible light; Oxidant; TiO_2; Hydroxyl radical; Photogenerated electron

1. Introduction

With the growth of urbanization and industrialization, the purification of wastewater containing contaminants has been a serious challenge in the environmental science and engineering fields. Unlike conventional methods, advanced oxidation processes (AOPs) are more effective in degrading the most recalcitrant pollutants into biodegradable compounds, by mainly relying on formation of highly reactive oxygen species (ROS) [1]. Furthermore, AOPs can avoid the problems of secondary contamination and salting resulting from the residuals (sludge, brines, and toxic waste) of conventional wastewater treatments [2]. Of many different AOPs, titanium dioxide (TiO_2) photocatalysis has been the most widely studied and used to degrade various organic contaminants [3–10] due to its chemical stability, long durability, nontoxicity, low cost, etc.

The detailed mechanism of TiO_2 photocatalysis has been discussed previously in numerous studies [11–15]. It is well established that the photocatalytic property is derived from the formation of photogenerated charge carriers (hole and electron), which occurs upon the absorption of illumination with the energy greater than TiO_2 band gap energy (3.2 eV) (Eq. (1)). The photogenerated holes and electrons may

* Corresponding author.

Presented at the 9th International Conference on Challenges in Environmental Science & Engineering (CESE-2016), 6–10 November 2016, Kaohsiung, Taiwan.

recombine unless they react with the species adsorbed on the surface of TiO_2 particles. The holes on valence band (h^+_{VB}) can oxidize organic matters directly, and react with water and hydroxyl ions to form hydroxyl radicals (•OH) (Eqs. (2)–(4)). The electrons on conduction band (e^-_{CB}) can reduce oxygen molecules to generate several types of ROS, such as superoxide anion (O_2•$^-$), hydroperoxyl radicals (HO_2•), and subsequently hydrogen peroxide (H_2O_2) as the precursors of •OH (Eqs. (5)–(12)). These generated ROS not only react with organics but also react with any present ROS, due to their nonselectivity (Eqs. (13)–(16)). As the target organic pollutant reacts with ROS, the purpose of pollutant removal can be reached by an oxidative decomposition process (Eq. (17)).

$$TiO_2 + h\nu(UV) \rightarrow TiO_2\ (e^-_{CB} + h^+_{VB}) \quad (1)$$

Oxidization on VB site:

$$h^+_{VB} + \text{organics} \rightarrow \text{degradation products} \quad (2)$$

$$h^+_{VB} + H_2O \rightarrow H_2O\bullet^+ \rightarrow \bullet OH + H^+ \quad (3)$$

$$h^+_{VB} + OH^- \rightarrow \bullet OH \quad (4)$$

Reduction on CB site:

$$e^-_{CB} + O_2 \rightarrow O_2\bullet^- \quad (5)$$

$$e^-_{CB} + O_2 + H^+ \rightarrow HO_2\bullet \quad (6)$$

$$e^-_{CB} + HO_2\bullet + H^+ \rightarrow H_2O_2 \quad (7)$$

$$e^-_{CB} + H_2O_2 \rightarrow \bullet OH + OH^- \quad (8)$$

$$H_2O_2 + h\nu(UV) \rightarrow 2\bullet OH \quad (9)$$

$$2O_2\bullet^- + 2H_2O \rightarrow 2\bullet OH + 2OH^- + O_2 \quad (10)$$

$$2O_2\bullet^- + 2H_2O \rightarrow 2H_2O_2 + O_2 \quad (11)$$

$$O_2\bullet^- + H_2O_2 \rightarrow \bullet OH + OH^- + O_2 \quad (12)$$

Between any two ROS:

$$\bullet OH + H_2O_2 \rightarrow HO_2\bullet + H_2O \quad (13)$$

$$\bullet OH + \bullet OH \rightarrow H_2O_2 \quad (14)$$

$$\bullet OH + O_2\bullet^- \rightarrow OH^- + O_2 \quad (15)$$

$$\bullet OH + HO_2\bullet \rightarrow H_2O + O_2 \quad (16)$$

$$\text{Organics} + h^+_{VB}, \bullet OH, O_2\bullet^-, HO_2\bullet \rightarrow \text{degradation products} \rightarrow CO_2 + H_2O \quad (17)$$

From the above, it is evident that the important roles in TiO_2 photocatalytic degradation process are the generated ROS especially •OH [16,17]. Differing from the past studies by using target pollutant removal, several techniques have been developed to detect •OH formation as the evaluation of photocatalytic activity. These techniques include electron spin resonance [18–21], luminescence [22], and fluorescence with terephthalic acid or coumarin (COU) as a probe molecule [16,17,23–25]. However, so far, the possible trends of •OH formation from VB and CB sites are not well explained.

Moreover, there is another problem about the actual application of TiO_2 photocatalysis, and it is hard to work under visible light (Vis) because of its limitation in band gap. In other words, TiO_2 has to be irradiated by ultraviolet (UV) light with enough energy to produce photocatalytic process. Unfortunately, only about 5%–7% of UV is covered in solar irradiance (46% Vis and 47% infrared radiation) [26]. In order to make use of the vast potential of solar photocatalysis, various techniques have been adopted such as surface modification [27,28], semiconductor coupling [29,30], doping of metals or nonmetals [31–34], adding of oxidizing agents into the aqueous TiO_2 suspensions [35,36], etc. Among the techniques mentioned above, the use of the oxidant, potassium dichromate ($K_2Cr_2O_7$, Cr(VI)), is simpler and more directly improves the degradation of organic pollutants by Vis-driven TiO_2 photocatalysis as reported previously [37]. In the meantime, the toxic Cr(VI) can be reduced to innocuous Cr(III) when Cr(VI) serves as electron scavenger to capture photogenerated electrons [38]. Hence, there is no doubt about secondary contamination.

Although investigations into the effects of various oxidants on degradation of organics have been executed, little work is performed to quantitatively characterize the simultaneous •OH formation from the combination of oxidants and TiO_2 photocatalysis. In this study, in order to quantify the assistances of oxidants in organic degradation and •OH formation by TiO_2 photocatalysis, two oxidants Cr(VI) and potassium permanganate ($KMnO_4$, Mn(VII)) were combined with TiO_2 for the degradation of azo dye acid orange 7 (AO7) as a target pollutant. Moreover, the photoformed •OH was measured under the different conditions, such as irradiation wavelengths (UV and Vis) and dissolved oxygen (DO) levels (aerobic and anoxic states). Based on the variation of photoformed •OH, the possible trends of •OH formation were inferred and proposed. This work could provide more detailed understanding of TiO_2 photocatalytic mechanism to extend the applicability and utility with solar light.

2. Materials and methods

2.1. Reagents and chemicals

A mixed-phase TiO_2 (Degussa P25) containing approximately 80% anatase and 20% rutile was used in this study. The target pollutant, dye AO7 was obtained from Panreac Co., Spain, and its properties are summarized as follows: molecular formula = $C_{16}H_{11}N_2NaO_4S$, λ_{max} = 485 nm, and molecular weight = 350.32 g/mol. Two oxidants, Cr(VI) and Mn(VII) were obtained from Hayashi Pure Chemical Ind., Ltd. (Osaka, Japan) and Katayama Chemical Ind. Co., Ltd. (Osaka, Japan), respectively. The adjustment of pH value was made by hydrogen chloride (HCl) and sodium hydroxide (NaOH) from Merck Co. (Darmstadt, Germany). Sodium sulfite (Na_2SO_3) was also manufactured by Hayashi Pure Chemical Ind., Ltd. to remove DO in our systems. COU

as •OH scavenger and its fluorescent product 7-hydroxycoumarin (7HC) were supplied from Alfa Aesar Co., Ltd. (Lancashire, United Kingdom).

2.2. Photocatalytic experiments for AO7 degradation

All of the experimental suspensions were prepared by using 100 μM of dye AO7 and 0.1 g of TiO_2 particles in deionized water placed in 200 mL Pyrex flask. The pH value of suspension was adjusted to 3.0 by HCl and NaOH, and then the suspension was thoroughly stirred in darkness for 30 min to reach an equilibrium (noted as 0 h). Prior to UV or Vis irradiation, 100 μM of oxidant was added into the suspension. The irradiation apparatuses used in this study were three UV (254 nm, 30 W, VL-330G, Vilber Lourmat, France) and Vis lamps (550 nm, 30 W, FL30Y, China Electric MFG Co., Taiwan), respectively. The irradiated distance was about 25 cm from the lamps to the suspension with an average luminous intensity at 25 Lux. At given time intervals, the appropriate amount of sample was collected and filtered through a microfiber filter (0.45 μm) to remove TiO_2 particles. For the evaluations of decolorization and mineralization, the differences of absorbance and total organic carbon (TOC) were analyzed by a spectrophotometer (Thermo Scientific Genesys 20) and a TOC analyzer (TOC-L CSH, Shimadzu), respectively. In addition, for the anoxic state, Na_2SO_3 was poured into the suspension to reduce DO below 0.1 mg/L (natural DO is about 7 mg/L). The DO concentration was measured by a portable multiparameter water quality meter (Bante903P, China).

2.3. Detection of hydroxyl radicals

The formation of •OH was quantitatively measured by the fluorescence probe technique with COU. In the measurement, all of the experimental parameters were the same to those in the AO7 photodegradation experiment, except AO7 was replaced with COU as •OH scavenger. The initial concentration of COU was 10^{-2} M, and 10^{-4} M of additional dosage was poured into the suspension during photocatalytic process to ensure the complete capture of •OH. As 1 mol of COU reacted with 2 mol of •OH, several hydroxycoumarin species would be formed, such as 7HC, 6HC, 5HC, and so on. Among these hydroxyl products, 7HC has a highly fluorescent property but its yield is only about 29% [39,40]. In addition, the reaction efficiency of COU with •OH was estimated by actual operations, which was around 6.42%. This estimated value was based on the difference between amounts of the theoretical •OH and measured •OH formations in the reaction of H_2O_2 and UV. Considering the above, the formation of •OH in TiO_2 photocatalytic process could be calculated from the concentration of 7HC by following correlation in Eq. (18).

$$C_{OH} = \frac{2}{0.29 \times 0.0642} \times C_{7HC} \quad (18)$$

The concentration of 7HC was analyzed to observe its fluorescent intensity at 450 nm by a fluorescence spectrophotometer (Hitachi F-4500, Japan) with the emission spectrum excited at 332 nm. To convert fluorescence intensity into actual concentration, the different concentrations of 7HC were analyzed as a standard curve. The above experiments including photodegradation of AO7 and fluorescence detection of •OH were replicated three times for the precision of experimental results.

3. Results and discussion

3.1. Effect of irradiation wavelength

As the first step of photocatalytic process, photocatalysts absorbed luminous energy to excite the separation of holes and electrons, and the absorbable range of illumination wavelength depended on their band gap energies. The band gap energy of TiO_2 (P25) is about 3.2 eV, and its absorbable wavelength shall be smaller than 385 nm which means UV region. In other words, the photocatalytic process would not function effectively under Vis irradiation. As shown in Fig. 1, the significant difference of AO7 mineralization between the different irradiation wavelengths was obtained. A little AO7 mineralization (about 10%) was found under constant darkness, although there was no catalytic result. The phenomenon may have originated from some negative AO7 molecules adsorbed on the positive surface of TiO_2 particles at the acidic pH condition [41], and the adsorption equilibrium would be reached within 30 min. Under UV irradiation, the mineralization of AO7 increased with increasing reaction time, and reached to 32% after 6 h. By deducting the adsorption removal from final mineralization, there was a contribution of 22% mineralization to be remained, which was the photocatalytic effect by UV light inducing. The mineralization efficiency contributed by Vis-induced photocatalysis was 11% after 6 h, hence it was known that the effect of irradiation wavelength on the photodegradation of AO7 was 11%.

Between UV and Vis irradiations, the decrease in AO7 mineralization could be attributed to the reduction of •OH formation, due to TiO_2 absorbed unsuitable luminous energy to lessen the photogenerated holes and electrons. Fig. 2 exhibits the photocatalytic formations of •OH under different irradiation wavelengths. The formations of •OH increased with extending reaction time both under UV and Vis irradiations,

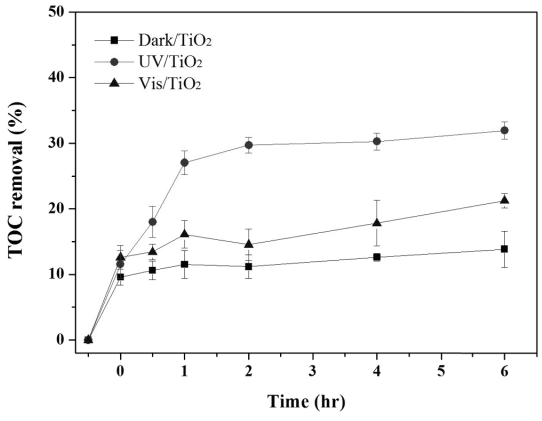

Fig. 1. Effect of irradiation wavelength on the AO7 mineralization by using TiO_2 photocatalysis.

and they were up to 68 × 10^{-6} M and 30 × 10^{-6} M after 6 h, respectively. Due to the effect of irradiation wavelength, the percentage difference of •OH formations was 56%.

3.2. Effect of oxidants Cr(VI) and Mn(VII)

It has been reported that oxidants not only possess oxidizing properties to degrade organics but also play the role of electron acceptor to inhibit hole–electron recombination, and further to improve TiO_2 photocatalytic activity [35,36]. In order to prove the effects of Cr(VI) and Mn(VII) on the photodegradation of AO7, they alone were used to degrade AO7. As shown in Fig. 3, the results show that decolorization efficiencies after 6 h were about 16% and 37% by Cr(VI) and Mn(VII), respectively. The oxidants Cr(VI) and Mn(VII) were useful for decolorization but useless for mineralization (Fig. 4). This might be because the decolorization of AO7 just represents the dissociation of azo chromophore (–N=N–) on AO7 molecule [42], hence it needs stronger oxidation performance that is enough to achieve mineralization. Although Cr(VI) and Mn(VII) alone could not degrade AO7 effectively, the degradations of AO7 under Vis irradiation were indeed improved in the presence of oxidants as shown in Fig. 4. The AO7 mineralization efficiencies were 27% for TiO_2/Cr(VI) and 39% for TiO_2/Mn(VII), and the improvements by Cr(VI) and Mn(VII) were about 6% and 18%, respectively (21% mineralization efficiency for TiO_2 alone).

Based on the above evidences, it could be deduced that the improvement of AO7 photodegradation was contributed from the enhancement of •OH formation by adding oxidant. We previously proved the effort of Cr(VI) to enhance •OH formation in TiO_2 photocatalytic process but lacked for the quantitative results [37]. In this study, the photoformed •OH from the combination of TiO_2 and oxidant under Vis irradiation was quantified. It was obvious that the •OH formations in the presence of Cr(VI) and Mn(VII) were higher than that in the absence of oxidant, as shown in Fig. 5. After 6 h, the •OH formations were about 30 × 10^{-6} M for TiO_2 alone, 37 × 10^{-6} M for TiO_2/Cr(VI), and 43 × 10^{-6} M for TiO_2/Mn(VII). The enhancements of •OH formation by Cr(VI) and Mn(VII) were about 26% and 44%, respectively.

3.3. Effect of dissolved oxygen

Fig. 6 demonstrates the difference in AO7 mineralization between aerobic and anoxic conditions by UV-induced TiO_2 photocatalysis. After 6 h, the mineralization efficiencies at aerobic condition were 32% (TiO_2 alone), 39% (TiO_2/Cr(VI)), and 46% (TiO_2/Mn(VII)) as shown in Fig. 6(a). Some researches have indicated the role of DO in photodegradation process is important because oxygen is necessary for complete mineralization [43,44]. Unsurprisingly, the AO7 mineralization efficiencies were decreased due to the absence of oxygen, which were 18% (TiO_2 alone), 22% (TiO_2/Cr(VI)), and 25% (TiO_2/Mn(VII)) as shown in Fig. 6(b). There was 15%–20% difference in AO7 mineralization between aerobic and anoxic conditions, and the value was slightly higher than that between the different wavelengths (11%). It seemed to represent the influence degree of oxygen was more important than that of irradiation wavelength. The reason might be that oxygen not only directly involves the mineralization of organics but also has other functions on the photocatalytic formation of ROS [2]. As adsorbed oxygen on TiO_2 surface acted an electron acceptor, several intermediates of •OH such as O_2•$^-$, HO_2•, and H_2O_2 would be produced from the reaction of oxygen and electron.

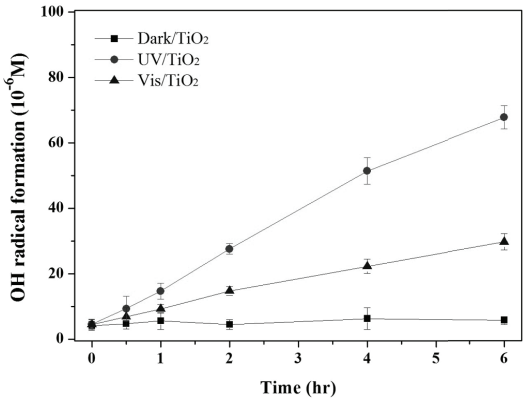

Fig. 2. Effect of irradiation wavelength on the •OH formation by using TiO_2 photocatalysis.

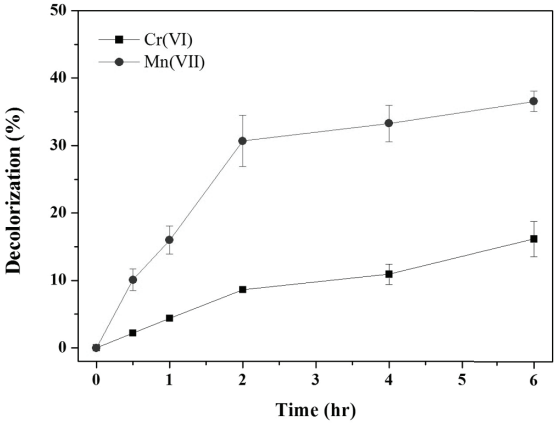

Fig. 3. Decolorization of AO7 by oxidants Cr(VI) and Mn(VII).

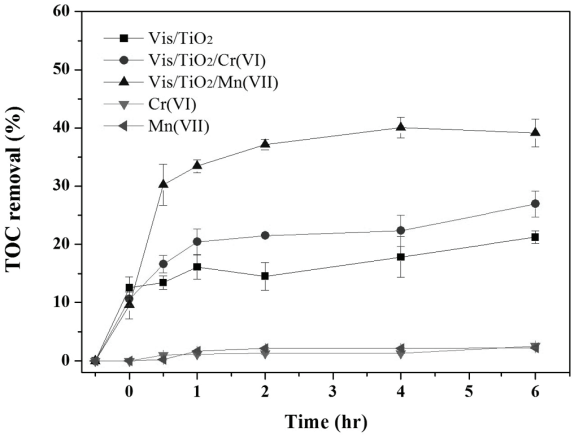

Fig. 4. AO7 mineralization varied by oxidant addition in TiO_2 photocatalytic process under Vis irradiation.

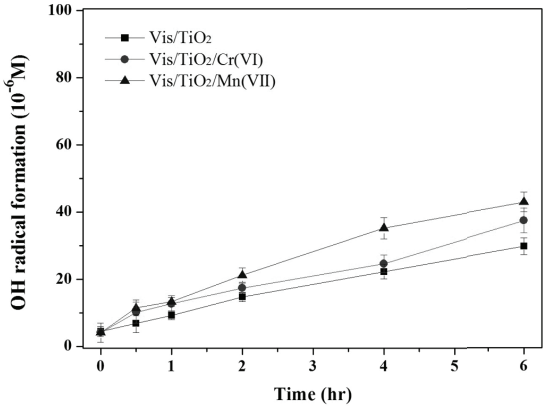

Fig. 5. Concentration of photoformed •OH varied by oxidant addition in TiO_2 photocatalytic process under Vis irradiation.

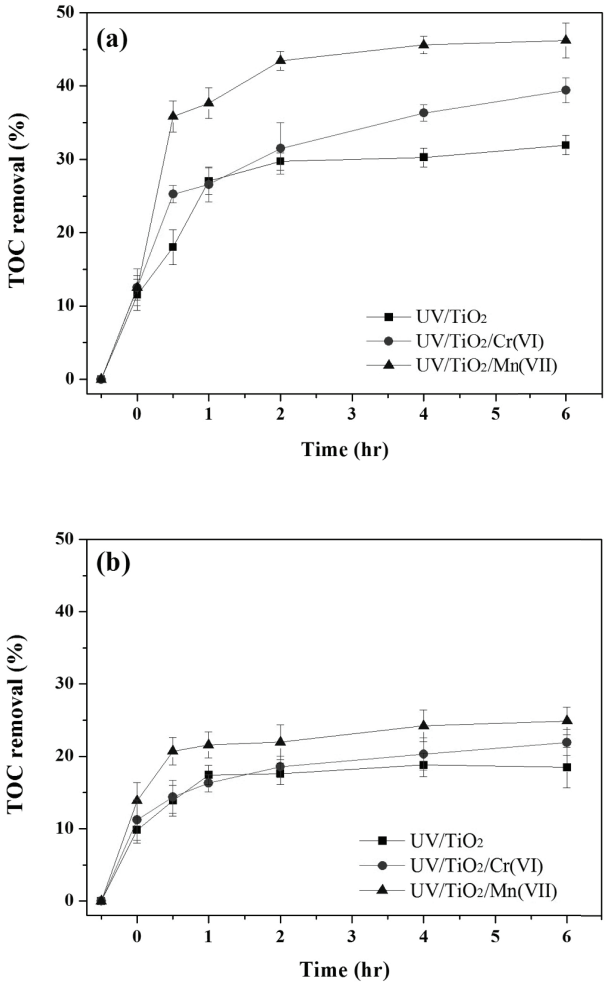

Fig. 6. Difference of AO7 mineralizations by TiO_2 alone and the combination of TiO_2 and oxidant under UV irradiation between (a) aerobic and (b) anoxic states.

Fig. 7 shows the •OH formations in UV-induced TiO_2 photocatalysis under the different conditions of DO. After 6 h, the •OH formations at aerobic state were 68 × 10^{-6} M

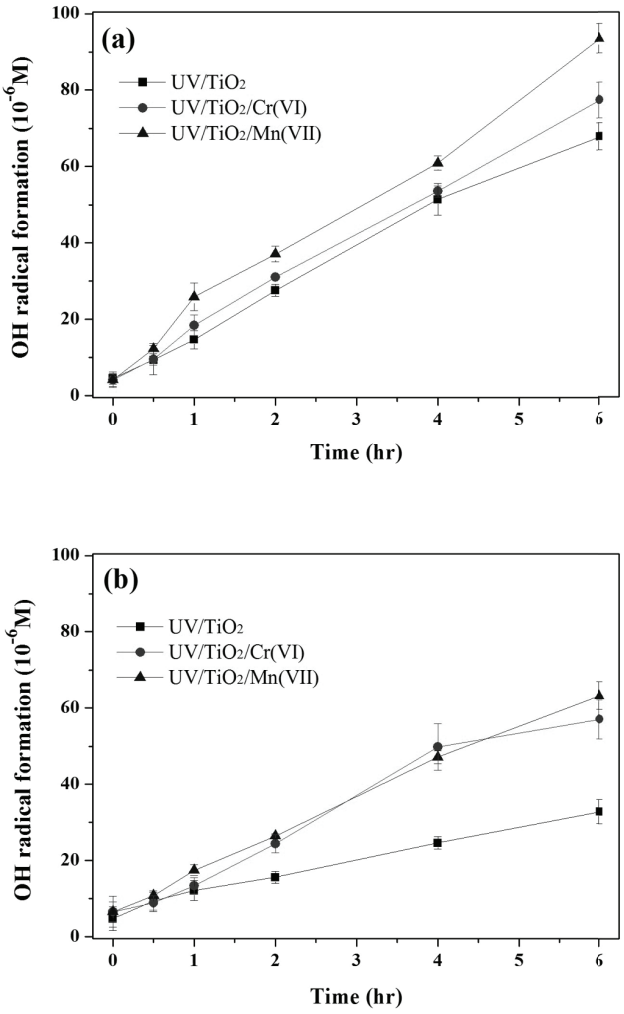

Fig. 7. Difference of •OH formations by TiO_2 alone and the combination of TiO_2 and oxidant under UV irradiation between (a) aerobic and (b) anoxic states.

(TiO_2 alone), 77 × 10^{-6} M (TiO_2/Cr(VI)), and 94 × 10^{-6} M (TiO_2/Mn(VII)), respectively (Fig. 7(a)). The •OH formations at anoxic state were obviously decreased to 33 × 10^{-6} M (TiO_2 alone), 57 × 10^{-6} M (TiO_2/Cr(VI)), and 63 × 10^{-6} M (TiO_2/Mn(VII)), respectively (Fig. 7(b)). There was 52% difference in •OH formation for TiO_2 alone, while the differences were 26% for TiO_2/Cr(VI) and 31% for TiO_2/Mn(VII). It implied that both Cr(VI) and Mn(VII) could reduce the loss of •OH formation caused by the absence of oxygen, probably because the oxidant also captured electrons to inhibit the recombination of hole–electron, and further to form more •OH.

3.4. Relationship between AO7 mineralization and •OH formation

Table 1 summarizes the mineralization efficiencies of AO7 and the concentrations of photoformed •OH in various photocatalytic systems with the different conditions. In order to understand the relationship between AO7 mineralization and •OH formation, the AO7 mineralizations were plotted as

Table 1
Summarization of AO7 mineralizations and •OH formations at 6 h photocatalytic processes with different conditions

Experimental conditions		TiO_2 alone		TiO_2/Cr(VI)		TiO_2/Mn(VII)	
Irradiation wavelength	Dissolved oxygen level	AO7 mineralization (%)	•OH Formation (10^{-6} M)	AO7 mineralization (%)	•OH Formation (10^{-6} M)	AO7 mineralization (%)	•OH Formation (10^{-6} M)
UV	Aerobic	32.0	67.8	39.4	77.4	46.2	93.6
	Anoxic	18.5	32.8	21.9	57.1	24.9	63.3
Vis	Aerobic	21.3	29.8	26.9	37.4	39.1	42.9
	Anoxic	13.0	10.2	16.0	22.3	18.8	24.6

a function of •OH formations (Fig. 8). There was a high and positive correlation to be observed, and the coefficient (r) was 0.82. The perfect correlation could not be reached, probably due to the sampling and analyzing errors, and/or the partial mineralization contribution from other uncertain mechanism. In some reports, it is suggested that the direct oxidation ability of photogenerated holes may also be an influence on the degradation of organics. Ishibashi et al. [45] indicated that the yield of photogenerated holes was 5.7×10^{-2}, which was equivalent to the quantum yield of ordinary photocatalytic reactions (~10^{-2}). In addition, Zhang and Nosaka [46] found the production rate of CO_2 from the acetaldehyde decomposition using TiO_2 photocatalysis was larger than that of •OH formation by about 10^3 times. Therefore, they considered that organic pollutant would be degraded mainly via photogenerated holes, not via •OH. However, this study confirmed that •OH formation was relatively important to the photodegradation of AO7.

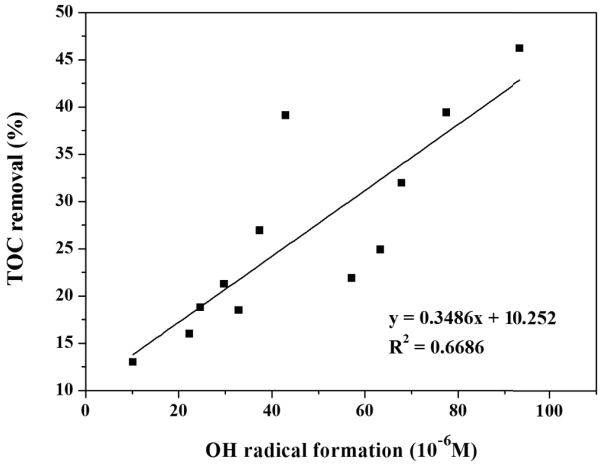

Fig. 8. Relationship between the AO7 mineralizations and •OH formations from different photocatalytic processes.

3.5. Formation trend of •OH and possible mechanism

After realizing the importance of •OH to the photodegradation of organics, its formation mechanism should be further clarified. According to the •OH formations under varying different conditions, the formation trends of •OH were estimated to establish possible mechanism. Generally, the source of photoformed •OH in TiO_2 photocatalytic process can be classified to two main portions, which are the oxidization on VB site and the reduction on CB site. There is only VB site to contribute the •OH formation at anoxic state, because oxygen only involves on CB site. Therefore, the contribution of •OH from CB site can be obtained from the difference in •OH formation between aerobic and anoxic conditions.

Based on the above, the formation trends of •OH by TiO_2 alone under different wavelength irradiations could be estimated as shown in Fig. 9. With UV irradiation, the percentages of photoformed •OH from VB (49%) and CB (51%) sites were nearly average. As TiO_2 was photocatalyzed by Vis irradiation, the percentage of total •OH formation decreased to 44% (relative to total •OH formation by UV irradiation). Furthermore, the percentages of photoformed •OH from VB and CB sites changed to 34% and 66%, respectively. It represented that advantage of •OH formation was toward CB site by the multipathways of •OH formation on CB site, if oxygen existed in the photocatalytic process.

The •OH formation trends and the possible mechanisms affecting the Cr(VI) and Mn(VII) are shown in Fig. 10. As

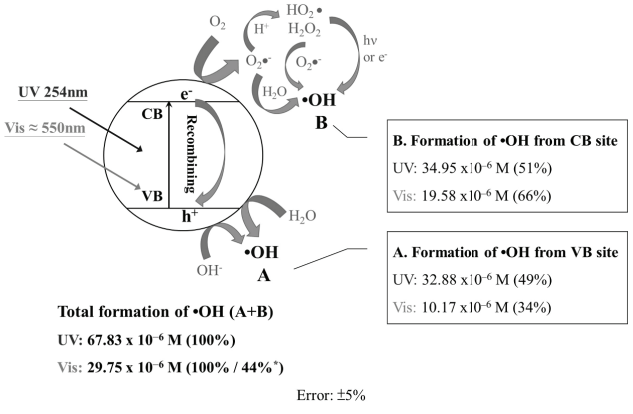

Fig. 9. Formation trends of •OH on TiO_2 reaction sites under UV and Vis irradiations. *Relative to the total •OH formation by TiO_2 alone.

Cr(VI) trapped photogenerated electrons, the •OH formation would be enhanced through its redox reaction, which was reported previously [37]. It was inferred that enhancement of •OH formation could be similarly achieved via the redox reaction of Mn(VII) and trapped electrons. The enhancements of •OH formation by Cr(VI) and Mn(VII) were 26% and 44% (relative to the total photoformed •OH by TiO_2

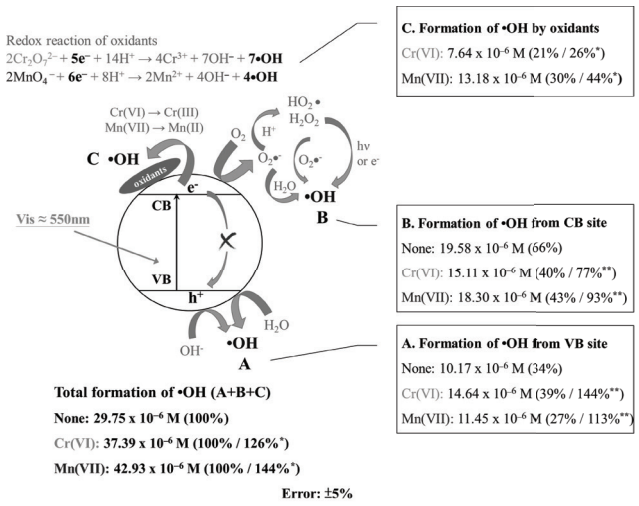

Fig. 10. Possible mechanisms of Cr(VI) and Mn(VII) for •OH formation improvement during Vis-driven TiO_2 photocatalytic process. *Relative to the total •OH formation by TiO_2 alone. **Relative to the •OH formation on the same site by TiO_2 alone.

alone), and were equivalent to 21% and 30% of the total •OH formations from TiO_2/Cr(VI) and TiO_2/Mn(VII), respectively. The •OH formation from CB site decreased since the partial photogenerated electrons were trapped to participate in the redox reaction of oxidants, but the CB site was still principal for •OH formation. The percentages of •OH formation on CB site were 40% and 43% for TiO_2/Cr(VI) and TiO_2/Mn(VII), respectively. In the meantime, the recombination of hole–electron was slightly inhibited to result in the increase of •OH formation from VB site, which were 144% and 113% for TiO_2/Cr(VI) and TiO_2/Mn(VII), respectively (relative to the •OH formation from VB site by TiO_2 alone).

The conventional strategies to improve Vis-driven activity of photocatalysts include the enhancement of lower energy photons absorbing and the inhibition of hole–electron recombining [47]. However, from the above mechanisms, it was evident that the addition of oxidants Cr(VI) and Mn(VII) in this study was dissimilar to the conventional strategies. The functions of Cr(VI) and Mn(VII) mainly increased the utilization of original photogenerated electrons to generate extra •OH by their redox reactions. In addition, Cr(VI) and Mn(VII) as electron scavengers could also inhibit the recombination of hole–electron to benefit photocatalytic activity. Thus, this study suggested that the use of oxidants would be an effective strategy to extend the applicability of TiO_2 photocatalysis with solar light.

4. Conclusions

This study investigated the effects of irradiation wavelength, oxidant addition, and DO level on the TiO_2 photocatalytic activities including AO7 photodegradation and •OH formation. Due to the reduction of generated holes and electrons in Vis-driven photocatalysis, the decreases in percentages of AO7 mineralization and •OH formation were 11% and 56%, respectively. The addition of oxidants was proved to improve the Vis-driven photocatalytic activity, and the improvements of Cr(VI) and Mn(VII) were 6% and 18% for AO7 mineralization, and 26% and 44% for •OH formation. In addition, the existence of oxygen in photocatalytic process was the most important factor because of its multiassistances in mineralization of organics and formation of ROS. Based on the variations of AO7 mineralization and •OH formation under different conditions, a highly positive correlation was observed. Moreover, the •OH formation trends from VB and CB sites on TiO_2 particles were estimated in this study, and they were quite near under UV irradiation. However, the key source of •OH formation transferred onto CB site (66%) under Vis irradiation, which was probably due to the effective reactivity of photogenerated electrons with oxygen. As Cr(VI) and Mn(VII) were similar to oxygen as electron acceptors, the utilization of photogenerated electrons could be further increased to form more •OH through their redox reactions. The extra •OH formations by Cr(VI) and Mn(VII) were equivalent to 21% and 30% in their respective composite processes. In the meantime, the partial recombination of hole–electron would also be inhibited, hence the •OH formation from VB site was enhanced. In summary, the use of oxidants in TiO_2 photocatalysis was an effective strategy to expand the applicability with solar light, and the mechanism was slightly different from the general strategies reported previously.

References

[1] M.N. Chong, B. Jin, C.W. Chow, C. Saint, Recent developments in photocatalytic water treatment technology: a review, Water Res., 44 (2010) 2997–3027.
[2] S. Malato, P. Fernández-Ibáñez, M.I. Maldonado, J. Blanco, W. Gernjak, Decontamination and disinfection of water by solar photocatalysis: recent overview and trends, Catal. Today, 147 (2009) 1–59.
[3] I.K. Konstantinou, T.A. Albanis, TiO_2-assisted photocatalytic degradation of azo dyes in aqueous solution: kinetic and mechanistic investigations: a review, Appl. Catal., B, 49 (2004) 1–14.
[4] U.I. Gaya, A.H. Abdullah, Heterogeneous photocatalytic degradation of organic contaminants over titanium dioxide: a review of fundamentals, progress and problems, J. Photochem. Photobiol., C, 9 (2008) 1–12.
[5] L. Mansouri, L. Bousselmi, Degradation of diethyl phthalate (DEP) in aqueous solution using TiO_2/UV process, Desal. Wat. Treat., 40 (2012) 63–68.
[6] K. Nakata, A. Fujishima, TiO_2 photocatalysis: design and applications, J. Photochem. Photobiol., C, 13 (2012) 169–189.
[7] V. Mahmoodi, J. Sargolzaei, Optimization of photocatalytic degradation of naphthalene using nano-TiO_2/UV system: statistical analysis by a response surface methodology, Desal. Wat. Treat., 52 (2014) 6664–6672.
[8] R.R. Kalantary, Y. Dadban Shahamat, M. Farzadkia, A. Esrafili, H. Asgharnia, Photocatalytic degradation and mineralization of diazinon in aqueous solution using nano-TiO_2 (Degussa, P25): kinetic and statistical analysis, Desal. Wat. Treat., 55 (2015) 555–563.
[9] T. Kaur, A.P. Toor, R.K. Wanchoo, Parametric study on degradation of fungicide carbendazim in dilute aqueous solutions using nano TiO_2, Desal. Wat. Treat., 54 (2015) 122–131.
[10] L. Mao, J. Shen, X. Ma, Z. Lan, X. Zhang, Effects of operational parameters on the photodegradation of 2,4-dinitrophenol in TiO_2 dispersion, Desal. Wat. Treat., 56 (2015) 744–751.
[11] A. Fujishima, T.N. Rao, D.A. Tryk, Titanium dioxide photocatalysis, J. Photochem. Photobiol., C, 1 (2000) 1–21.
[12] N. San, A. Hatipoğlu, G. Koçtürk, Z. Çınar, Photocatalytic degradation of 4-nitrophenol in aqueous TiO_2 suspensions: theoretical prediction of the intermediates, J. Photochem. Photobiol., A, 146 (2002) 189–197.

[13] U.G. Akpan, B.H. Hameed, Parameters affecting the photocatalytic degradation of dyes using TiO_2-based photocatalysts: a review, J. Hazard. Mater., 170 (2009) 520–529.
[14] W. Li, D. Li, Y. Lin, P. Wang, W. Chen, X. Fu, Y. Shao, Evidence for the active species involved in the photodegradation process of methyl orange on TiO_2, J. Phys. Chem. C, 116 (2012) 3552–3560.
[15] W.Y. Teoh, J.A. Scott, R. Amal, Progress in heterogeneous photocatalysis: from classical radical chemistry to engineering nanomaterials and solar reactors, J. Phys. Chem. Lett., 3 (2012) 629–639.
[16] H. Czili, A. Horváth, Applicability of coumarin for detecting and measuring hydroxyl radicals generated by photoexcitation of TiO_2 nanoparticles, Appl. Catal., B, 81 (2008) 295–302.
[17] Q. Xiang, J. Yu, P.K. Wong, Quantitative characterization of hydroxyl radicals produced by various photocatalysts, J. Colloid Interface Sci., 357 (2011) 163–167.
[18] T. Wu, T. Lin, J. Zhao, H. Hidaka, N. Serpone, TiO_2-assisted photodegradation of dyes. 9. Photooxidation of a squarylium cyanine dye in aqueous dispersions under visible light irradiation, Environ. Sci. Technol., 33 (1999) 1379–1387.
[19] W. Zhao, C. Chen, X. Li, J. Zhao, H. Hidaka, N. Serpone, Photodegradation of sulforhodamine-B dye in platinized titania dispersions under visible light irradiation: influence of platinum as a functional co-catalyst, J. Phys. Chem. B, 106 (2002) 5022–5028.
[20] W. Li, D. Li, J. Xian, W. Chen, Y. Hu, Y. Shao, X. Fu, Specific analyses of the active species on $Zn_{0.28}Cd_{0.72}S$ and TiO_2 photocatalysts in the degradation of methyl orange, J. Phys. Chem. C, 114 (2010) 21482–21492.
[21] Z. Wang, W. Ma, C. Chen, H. Ji, J. Zhao, Probing paramagnetic species in titania-based heterogeneous photocatalysis by electron spin resonance (ESR) spectroscopy – a mini review, Chem. Eng. J., 170 (2011) 353–362.
[22] C.H. Tsai, A. Stern, J.F. Chiou, C.L. Chern, T.Z. Liu, Rapid and specific detection of hydroxyl radical using an ultraweak chemiluminescence analyzer and a low-level chemiluminescence emitter: application to hydroxyl radical-scavenging ability of aqueous extracts of food constituents, J. Agric. Food. Chem., 49 (2001) 2137–2141.
[23] K.I. Ishibashi, A. Fujishima, T. Watanabe, K. Hashimoto, Detection of active oxidative species in TiO_2 photocatalysis using the fluorescence technique, Electrochem. Commun., 2 (2000) 207–210.
[24] T. Hirakawa, K. Yawata, Y. Nosaka, Photocatalytic reactivity for O_2^- and OH radical formation in anatase and rutile TiO_2 suspension as the effect of H_2O_2 addition, Appl. Catal., A, 325 (2007) 105–111.
[25] J. Yu, W. Wang, B. Cheng, B.L. Su, Enhancement of photocatalytic activity of mesporous TiO_2 powders by hydrothermal surface fluorination treatment, J. Phys. Chem. C, 113 (2009) 6743–6750.
[26] T. Bak, J. Nowotny, M. Rekas, C.C. Sorrell, Photo-electrochemical hydrogen generation from water using solar energy. Materials-related aspects, Int. J. Hydrogen Energy, 27 (2002) 991–1022.
[27] D. Chatterjee, A. Mahata, Photoassisted detoxification of organic pollutants on the surface modified TiO_2 semiconductor particulate system, Catal. Commun., 2 (2001) 1–3.
[28] D. Jiang, Y. Xu, D. Wu, Y. Sun, Visible-light responsive dye-modified TiO_2 photocatalyst, J. Solid State Chem., 181 (2008) 593–602.
[29] L. Wu, C.Y. Jimmy, X. Fu, Characterization and photocatalytic mechanism of nanosized CdS coupled TiO_2 nanocrystals under visible light irradiation, J. Mol. Catal. A: Chem., 244 (2006) 25–32.
[30] W. Ho, C.Y. Jimmy, Sonochemical synthesis and visible light photocatalytic behavior of CdSe and CdSe/TiO_2 nanoparticles, J. Mol. Catal. A: Chem., 247 (2006) 268–274.
[31] R. Asahi, T. Morikawa, T. Ohwaki, K. Aoki, Y. Taga, Visible-light photocatalysis in nitrogen-doped titanium oxides, Science, 293 (2001) 269–271.
[32] J.C. Yu, J. Yu, W. Ho, Z. Jiang, L. Zhang, Effects of F-doping on the photocatalytic activity and microstructures of nanocrystalline TiO_2 powders, Chem. Mater., 14 (2002) 3808–3816.
[33] B. Xin, P. Wang, D. Ding, J. Liu, Z. Ren, H. Fu, Effect of surface species on Cu-TiO_2 photocatalytic activity, Appl. Surf. Sci., 254 (2008) 2569–2574.
[34] L.G. Devi, N. Kottam, B.N. Murthy, S.G. Kumar, Enhanced photocatalytic activity of transition metal ions Mn^{2+}, Ni^{2+} and Zn^{2+} doped polycrystalline titania for the degradation of Aniline Blue under UV/solar light, J. Mol. Catal. A: Chem., 328 (2010) 44–52.
[35] H. Kyung, J. Lee, W. Choi, Simultaneous and synergistic conversion of dyes and heavy metal ions in aqueous TiO_2 suspensions under visible-light illumination, Environ. Sci. Technol., 39 (2005) 2376–2382.
[36] H. Eskandarloo, A. Badiei, M.A. Behnajady, Study of the effect of additives on the photocatalytic degradation of a triphenylmethane dye in the presence of immobilized TiO_2/NiO nanoparticles: artificial neural network modeling, Ind. Eng. Chem. Res., 53 (2014) 6881–6895.
[37] Y.S. Wang, J.H. Shen, J.J. Horng, Chromate enhanced visible light driven TiO_2 photocatalytic mechanism on Acid Orange 7 photodegradation, J. Hazard. Mater., 274 (2014) 420–427.
[38] S.G. Schrank, H.J. José, R.F.P.M. Moreira, Simultaneous photocatalytic Cr(VI) reduction and dye oxidation in a TiO_2 slurry reactor, J. Photochem. Photobiol., A, 147 (2002) 71–76.
[39] G. Louit, S. Foley, J. Cabillic, H. Coffigny, F. Taran, A. Valleix, J.P. Renault, S. Pin, The reaction of coumarin with the OH radical revisited: hydroxylation product analysis determined by fluorescence and chromatography, Radiat. Phys. Chem., 72 (2005) 119–124.
[40] M. Tokumura, R. Morito, R. Hatayama, Y. Kawase, Iron redox cycling in hydroxyl radical generation during the photo-Fenton oxidative degradation: dynamic change of hydroxyl radical concentration, Appl. Catal., B, 106 (2011) 565–576.
[41] I.S. Grover, S. Singh, B. Pal, The preparation, surface structure, zeta potential, surface charge density and photocatalytic activity of TiO_2 nanostructures of different shapes, Appl. Surf. Sci., 280 (2013) 366–372.
[42] P. Bansal, D. Singh, D. Sud, Photocatalytic degradation of azo dye in aqueous TiO_2 suspension: reaction pathway and identification of intermediates products by LC/MS, Sep. Purif. Technol., 72 (2010) 357–365.
[43] W. Han, P. Zhang, W. Zhu, J. Yin, L. Li, Photocatalysis of *p*-chlorobenzoic acid in aqueous solution under irradiation of 254 nm and 185 nm UV light, Water Res., 38 (2004) 4197–4203.
[44] I. García-Fernández, I. Fernández-Calderero, M.I. Polo-López, P. Fernández-Ibáñez, Disinfection of urban effluents using solar TiO_2 photocatalysis: a study of significance of dissolved oxygen, temperature, type of microorganism and water matrix, Catal. Today, 240 (2015) 30–38.
[45] K.I. Ishibashi, A. Fujishima, T. Watanabe, K. Hashimoto, Quantum yields of active oxidative species formed on TiO_2 photocatalyst, J. Photochem. Photobiol., A, 134 (2000) 139–142.
[46] J. Zhang, Y. Nosaka, Quantitative detection of OH radicals for investigating the reaction mechanism of various visible-light TiO_2 photocatalysts in aqueous suspension, J. Phys. Chem. C, 117 (2013) 1383–1391.
[47] S. Rehman, R. Ullah, A.M. Butt, N.D. Gohar, Strategies of making TiO_2 and ZnO visible light active, J. Hazard. Mater., 170 (2009) 560–569.